

THEORY OF AUGER RECOMBINATION IN A QUANTUM WELL WIRE

R.I. TAYLOR, R.W. KELSALL and R.A. ABRAM

Department of Applied Physics and Electronics, University of Durham, Durham, DH1 3LE, UK

Received 30 July 1985; accepted for publication 14 October 1985

Calculations are presented for the rate of Auger recombination in a semiconductor quantum well wire. An expression is given for the rate of the CHSH Auger process in which the carriers remain in their ground subbands, and the rates of other processes such as CHCC may be obtained by simple algebraic substitution. Numerical calculations that consider all possible bound-to-bound intra- and inter-subband transitions are reported. Results are given for the rate of the CHCC process as a function of wire width and wire axis direction for an InGaAsP/InP quantum well wire.

1. Introduction

A quantum well wire (QWW) laser is expected to have a better gain spectrum than either a quantum well (QW) laser, or a conventional DH laser [1], and this should lead to lower and less-temperature-dependent threshold currents [2], provided there are no adverse effects from non-radiative recombination. However, for the long-wavelength lasers used in optical fibre communications systems, Auger recombination can be an important non-radiative process (with a possible significant influence on the threshold current), in both QW [3] and DH lasers [4]. Hence, an estimate of the Auger recombination rate in a QWW would not only provide more information about the Auger process, but would also help to determine whether or not a QWW laser will be a good device for optoelectronic applications.

The QWW is taken to have a square cross section of width L , and, for simplicity, the wavefunctions of the carriers are assumed to vanish outside the wire (i.e. the assumption is made that there is an infinite potential discontinuity at the wire edge). This approximation means that all carrier states are bound by the well. If the potential discontinuity were taken to be finite, which is the actual case, then carriers with sufficient energy could be above the top of the confining well, and these would be unbound states [5]. The Auger rate is calculated with the common assumptions of isotropic, parabolic bands and Boltzmann statistics with quasi-Fermi levels. These simplifying assumptions enable us to obtain an analytical result for the rate of the QWW equivalent of the CHSH Auger process. The analytical result obtained enables physical

insight into the Auger process in a QWW, which would not be obtained in a fully numerical calculation.

2. Analytical calculation of the CHSH Auger rate in a QWW

The band-to-band Auger recombination rate for the QWW equivalent of the CHSH process is calculated using Fermi's golden rule (the letters CHSH refer to the bands of the states involved in the Auger process) and is illustrated in fig. 1. Fermi's golden rule gives the rate per unit volume for the Auger process as:

$$R = \frac{1}{L^2 X} \frac{2\pi}{\hbar} \sum P_{\text{stat}} |M|^2 \delta(E_1 + E_2 - E_{1'} - E_{2'}), \quad (1)$$

where E_i is the energy of carrier i (see fig. 1), L the width of quantum well wire, X the length of wire, P_{stat} the statistical factor, and M the matrix element for the Auger process.

For the transition energies involved in the Auger processes for typical laser materials, it is reasonable to ignore free-carrier screening [6], and for the case

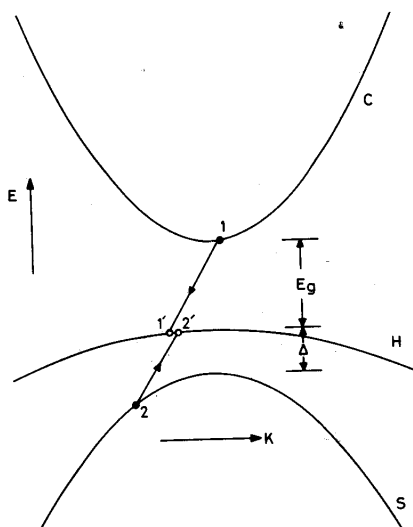


Fig. 1. The CHSH Auger process in the ground-state subbands of a quantum well wire (other subbands omitted for clarity).

where carriers have opposite spins separately conserved in the Auger process, the matrix element can be written in the form

$$M = \int \int \psi_1^*(\mathbf{r}_1) \psi_2^*(\mathbf{r}_2) \frac{e^2}{\epsilon |\mathbf{r}_1 - \mathbf{r}_2|} \psi_1(\mathbf{r}_1) \psi_2(\mathbf{r}_2) d^3\mathbf{r}_1 d^3\mathbf{r}_2. \quad (2)$$

Using the approximations outlined in section 1, the wavefunctions of the carriers may be written as:

$$\psi(\mathbf{r}) = \frac{2}{X^{1/2}L} \sin\left(\frac{n_y\pi y}{L}\right) \sin\left(\frac{n_z\pi z}{L}\right) e^{ik_x x} u_k(\mathbf{r}), \quad (3)$$

where $u_k(\mathbf{r})$ is the periodic part of the Bloch function.

Using these wavefunctions in (2), and $|M|^2$ in (1), and summing over all the states by taking the energy bands to be parabolic, leads to an expression for the CHSH Auger rate. For the case where the carriers reside in their ground-state subbands, the CHSH rate (for the case of opposite spins separately conserved and systems with $E_g > \Delta$) may be written as:

$$R = \frac{81\pi e^4}{4\epsilon^2 \hbar} \frac{p}{p_C} \left(\frac{np}{n_0 p_0} - 1 \right) \frac{|M^{\text{CH}}|^2 |M^{\text{HS}}|^2}{k_0^4 L^6} S^2(k_0 L / \pi) \times \left(\frac{a_s}{\mu_s^2 \mu_H (2 + \mu_H)} \right)^{1/2} \frac{1}{\beta \alpha^{3/2} \Delta E^{1/2}} \exp\left[-\beta \left(\Delta + \mu_s \frac{\Delta E}{a_s} \right) \right]. \quad (4)$$

The carrier densities are all per unit length of the wire, and p_C is the effective density of states of the hole subbands

$$p_C \approx (2m_H k_B T / \pi \hbar^2)^{1/2}.$$

$\Delta E = E_g - \Delta$ and the other symbols have their usual meanings [7]. The function S^2 (see fig. 2) arises as a correction factor to the wide-well-limit expression for the matrix element. (In the wide-well limit the matrix element is proportional to $k_0^{-2} L^{-2}$.)

For the region of well widths where the wide-well limit is a good approximation and also where the majority of carriers reside in their ground-state subbands, the QWW, QW and bulk Auger CHSH rates are related by [7]

$$\frac{R_{\text{QWW}}}{R_{\text{QW}}} = \frac{9}{4\pi^{1/2}} \frac{2m_H + m_C}{2m_H + m_C - m_S} \left(\frac{k_B T}{E_a} \right)^{1/2},$$

$$\frac{R_{\text{QW}}}{R_{\text{bulk}}} = \frac{9\pi^{1/2}}{8} \frac{2m_H + m_C}{2m_H + m_C - m_S} \left(\frac{k_B T}{E_a} \right)^{1/2},$$

where E_a is the activation energy for the CHSH process

$$E_a = \frac{m_S \Delta E}{2m_H + m_C - m_S}.$$

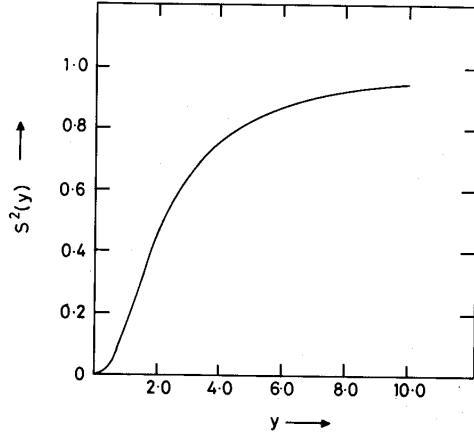


Fig. 2. A graph of $S^2(y)$ versus y . In the expression for the Auger rate $y = k_0 L / \pi$.

This may be seen from eq. (4) by assuming that $np \gg n_0 p_0$ and then noting that $n_0 p_0 \propto \exp(-E_g/k_B T)$.

The calculation may be extended to include Auger processes in which some of the carriers reside in or make transitions to excited subbands. It should be pointed out that not all possible intersubband transitions are allowed within the framework of the model. This occurs since the matrix element in eq. (2) can vanish for symmetry reasons. A similar situation was encountered in the QW case. In that case the selection rule was expressed mathematically in terms of the quantum numbers of the confined states, and the selection rule for allowed transitions was $n_1 + n_2 - n_{1'} - n_{2'} = \text{even}$. In the QWW, the carriers reside in subbands that are described by two quantum numbers (e.g., carrier in state $|1\rangle$ has quantum numbers n_{1y}, n_{1z}). In this case the allowed transitions have to satisfy $n_{1y} + n_{2y} - n_{1'y} - n_{2'y} = \text{even}$ and $n_{1z} + n_{2z} - n_{1'z} - n_{2'z} = \text{even}$.

3. Results

A simple change of parameters in eq. (4) can lead to results for rates of other direct band-to-band Auger processes. For example, if the following change of parameters is made: $\Delta = 0$, $m_S = m_H$, n and p permuted, and then m_C and m_H permuted, then eq. (4) will give the rate of the CHCC Auger process. Rates of other Auger processes, for example, CHHH, CHLH, CLSL, etc., can be evaluated from eq. (4) in a similar way. To demonstrate the influence of wire parameters on Auger transitions it is convenient to consider

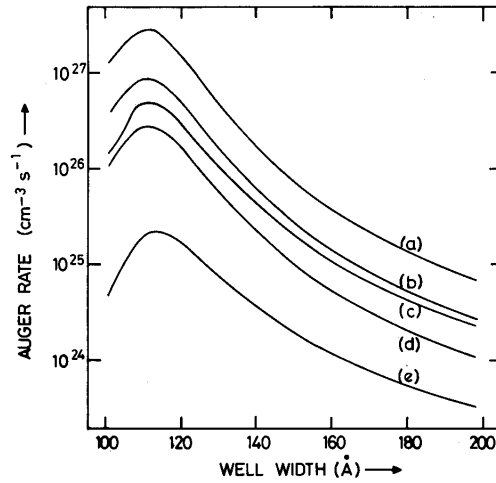


Fig. 3. A graph of the individual contributions to the CHCC Auger rate from various different intersubband transitions: (a) (11) (11) (11) (11), (b) (11) (11) (12) (12), (c) (11) (11) (13) (13), (d) (11) (11) (22) (22), (e) (11) (11) (13) (11), where the subband indices (n_y, n_z) are given for carriers $|1\rangle, |2\rangle, |1'\rangle, |2'\rangle$ respectively. The electron and hole concentrations are 10^{18} cm^{-3} and the temperature is 300 K.

the CHCC process which has the simplicity of involving only two types of carrier. This also facilitates a direct comparison with earlier work [5] on the quantum well system. Fig. 3 shows a plot of the CHCC Auger bound-bound rate as a function of L for various intersubband transitions.

The wavelength of the QWW laser is kept constant at $1.3 \mu\text{m}$ by ensuring that the energy separation of the ground-state conduction and heavy-hole subbands is constant at 0.95 eV. This is achieved by varying the composition of the InGaAsP whilst keeping it lattice matched to InP. The conduction- and valence-band quasi-Fermi levels are calculated in the usual way, with a sufficient number of subbands included to ensure convergence, and for all the results, an equal electron and hole concentration of 10^{18} cm^{-3} has been assumed. The maxima in fig. 3 are a consequence of a maximum in $(F_C - F_V)$, the difference between the conduction- and valence-band quasi-Fermi levels. Compositional constraints prevent us from considering well widths less than 100 Å since below this width, the subband separation of the ground-state conduction and heavy-hole subbands is always greater than 0.95 eV.

In the case of a QW, the CHCC bound-bound Auger rate was shown to have a "saw-tooth" variation with well width [5]. This is a direct consequence of the use of a finite potential discontinuity at the QW edge. For the QWW,

the assumption has been made of an infinite potential discontinuity at the wire edge, and so no "saw-tooth" variation is seen.

The results in fig. 3 are calculated for a wire axis in the [110] direction, using values for the overlap integrals of the Bloch functions from a pseudopotential calculation [8,9]. The Bloch functions are taken as those appropriate to the axial wavevectors of the threshold states and the transverse wavevectors due to confinement are ignored. In this approximation all Bloch functions are determined by wavevectors parallel to the wire axis, and for this case the results of ref. [8] show that the conduction/heavy-hole (CH) overlap is strongly dependent on wavevector direction whereas the conduction/conduction overlap is isotropic. This would seem to imply that there will be a strong variation in the CHCC Auger rate with wire axis direction reflecting the directional dependence of the CH overlap given by fig. 1 of ref. [8], and that the Auger rate will be very small for a wire axis in the [100] and [111] directions (see refs. [8-11]). However, the states do in fact have transverse wavevector components and these are substantial. Hence the wavevectors to be used in the overlap integrals are not parallel and consequently the true integrals and the Auger rate are expected to be much less dependent on the direction of the wire axis [9]. In particular, the Auger rate is unlikely to be very small for certain axial directions.

Acknowledgements

The authors would like to thank Dr. S. Brand for useful discussions and the numerical results for the overlap integrals. R.I. Taylor acknowledges tenure of a SERC CASE studentship in association with British Telecom Research Laboratories during the period of this work.

References

- [1] M. Asada, Y. Miyamoto and Y. Suematsu, Japan. J. Appl. Phys. 24 (1985) L95.
- [2] Y. Arakawa and H. Sakaki, Appl. Phys. Letters 40 (1982) 939.
- [3] C. Smith, R.A. Abram and M.G. Burt, Electron. Letters 20 (1984) 893.
- [4] C.B. Su, J. Schlafer, J. Mannig and R. Olshansky, Electron. Letters 18 (1982) 595.
- [5] C. Smith, R.A. Abram and M.G. Burt, Superlattices Microstructures 1 (1985) 119.
- [6] M.G. Burt, J. Phys. C. 14 (1981) 3269.
- [7] R.I. Taylor, R.A. Abram, M.G. Burt and C. Smith, IEE Proc. J. Optoelectron. 132 (1985) 364.
- [8] M.G. Burt, S. Brand, C. Smith and R.A. Abram, J. Phys. C17 (1984) 6385.
- [9] S. Brand, private communication.
- [10] M.G. Burt and C. Smith, J. Phys. C 17 (1984) L47.
- [11] M. Takeshima, Phys. Rev. B31 (1985) 992.